

MATHEMATICAL MODELS OF NEUROSCIENCE

MASTERS DEGREE IN BIOMEDICAL ENGINEERING

Project #2 - Data Analysis [EN]

Authors:

Afonso Araújo (10812300)
Letizia Rossato (10802300)

afonso.soares@student.uclouvain.be
letizia.rossato@student.uclouvain.be

2023/2024 – 1st Semester

1 Introduction

The following report is split in three sections. In the first section the group analyzed the firing rate of several subjects in a laboratory environment in order to draw conclusions regarding neuron's directional tuning. In the second section of the report the group correlated data from subject's pectoralis major and posterior deltoid EMGs with subject's hand kinematics and applied forces. In the last section, the group compared the one joint stochastic controller with neural data.

2 Neural Data Analysis

2.1 Firing Rate

A subject's firing rate was computed for the task of target reaching. The subject reached for eight targets six different times per target. The firing rate was computed for each trial through the convolution between a rectangular kernel and the spikes' pattern. Also as part of the data processing, the group aligned every joint and cartesian placement data to be coherent with the firing rate. In this way the group minimized the effect of the noise and removed the beginning wind up and overshoot of the end from the part of the subject.

The result was then averaged through every trial of one target, obtaining the mean firing rate for each target, as shown in figure 1.

2.2 Movement Kinematics and Directional Tuning

With the plot of the movements on the x-y plane, together with the mean firing rate, it's possible to observe the directional tuning of the cells.

From figure 1, some neural cell's directional tuning's features can be gauged. In the centre of the graph, it's represented the sequence of movements towards 8 targets, equidistant and evenly placed around a circle. The movements start from the centre of the circle and the patient completed 6 reaching movements for each target.

For each target, the mean firing rate is represented, near the target itself and with the same color pattern. All the graphs regarding the firing rate have the same scale on the frequency axis. In this way, it's easy to distinguish during which movements there was the highest neural activity.

The peak of spikes rate is reached during the execution of movements towards the third target. The firing rate during the reaching of targets #4 and #7 is particularly low.

Given these observations, the group concluded that the cells present some sort of diagonal directional tuning. Since targets #4 and #7 are the ones to the top left and bottom right, and #5 and #2 are the ones at top right and bottom left, there is some sort of diagonal cell feature.

When looking at shoulder/elbow evolution for targets #4, #7 and #5, #2, in figure 2, comparing them with the respective firing rates doesn't convey as much information regarding the directional tuning as it did when comparing hand coordinates, for these targets, with firing rates. This concludes that hand coordinates and firing rates are much more indicative of directional tuning than shoulder/elbow and firing rates.

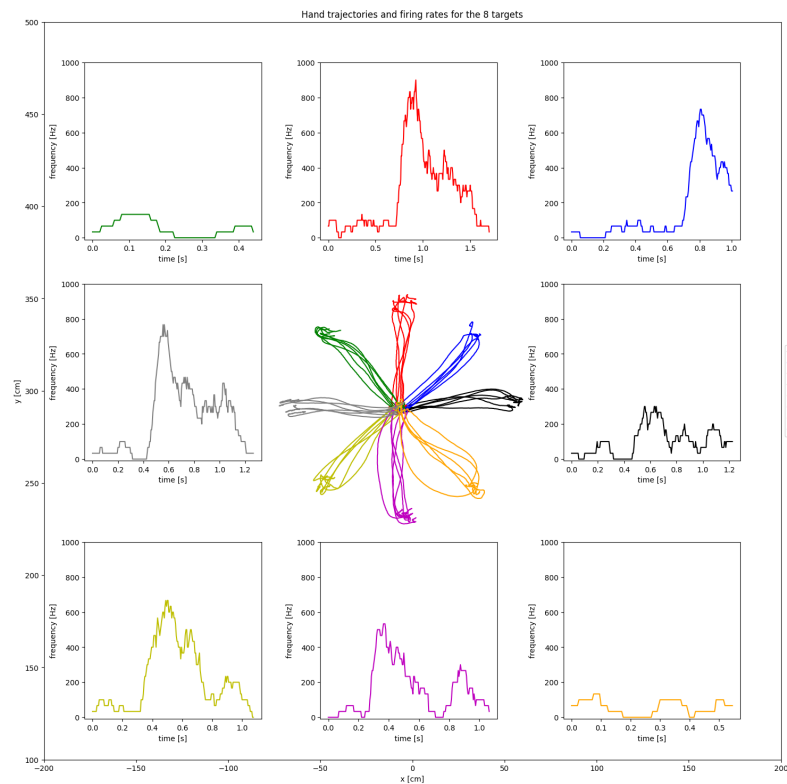


Figure 1: Subject's Hand Trajectories with respective Firing Rates

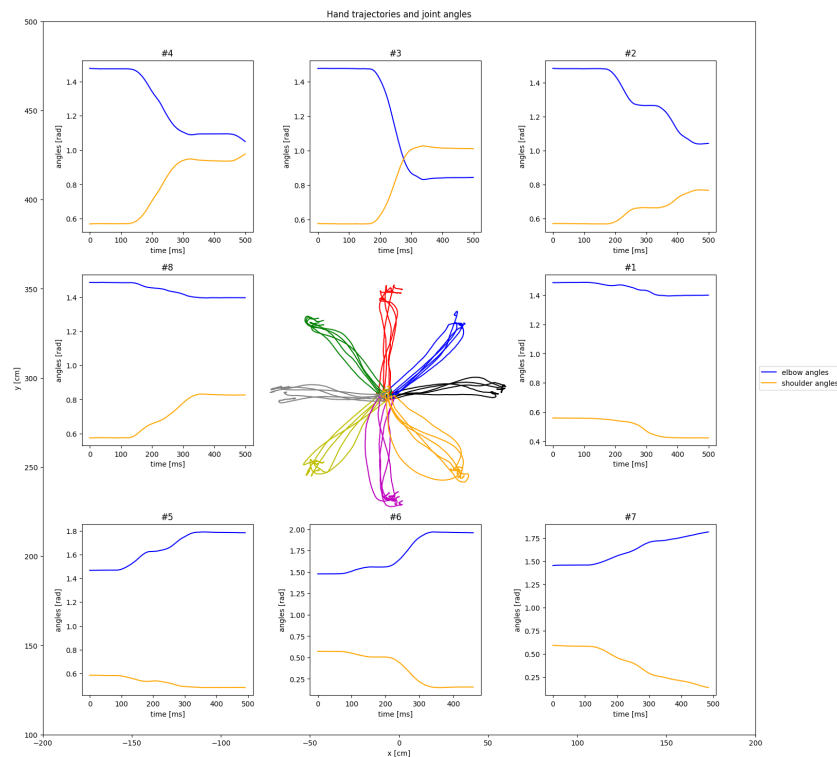


Figure 2: Subject's Hand Trajectories with Respective Joint Angles

3 EMG Data Analysis

For this section, the subject was instructed to reach a target positioned in front of him. The subject's arm was attached to a robotic exoskeleton that can apply a force to such arm directed to the right (**positive force**) or the left (**negative force**) of the patient, as shown in figure 3. This force was proportional to the subject's hand speed. It is assumed that the arm in question is the subject's right arm. In this chapter the group is going to compare both **Limb Kinematics** and **Subject's Force** with EMG data from the subject's pectoralis major and posterior deltoid muscles.

3.1 Relationship between EMG and Limb Kinematics

Below is the representation of subject's hand position for trial #1,

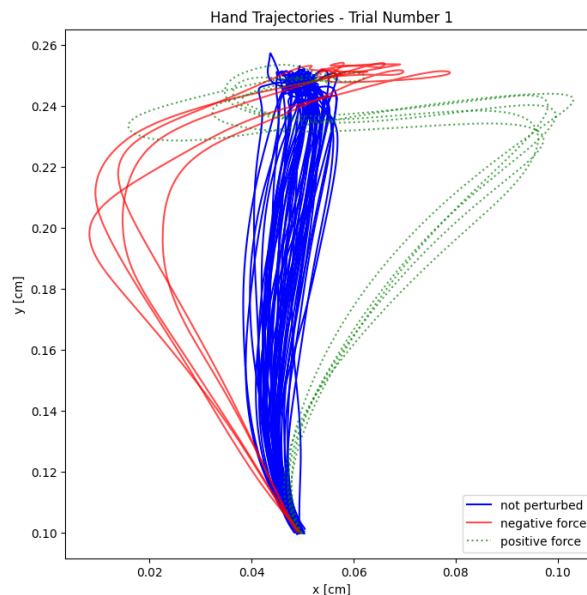


Figure 3: Subject's Hand Trajectories as recorded by the Robotical System

When the patient is subjected to a force, the patient's muscles work to counteract it in a way that the patient still reaches the proposed target. An adduction movement is defined as a decrease of the distance between the limb and the body, whereas abduction is the opposite - increase of the distance from the body.

Theoretically, always considering the right arm, the pectoralis should show a higher activity during adduction movements, because contracting it causes the arm to get closer to the body. On the opposite, the deltoid should play a more important role in movements of abduction. This was partially verified in figures 4 and 5, where the activity of the 2 muscles is shown for the first 400 ms of each aligned movement.

For the pectoralis, it's clearly shown that the muscle is more used in the case of **positive force**, with an activity increase from 100 ms from the beginning of the movement. In the case of **negative force**, the pectoralis helps the movement only after 300 ms, probably engaging for stabilizing reasons.

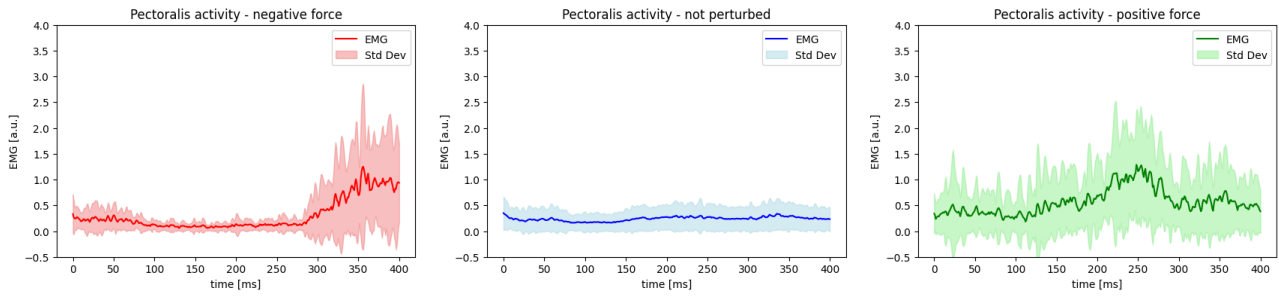


Figure 4: Pectoralis Major's EMG Data

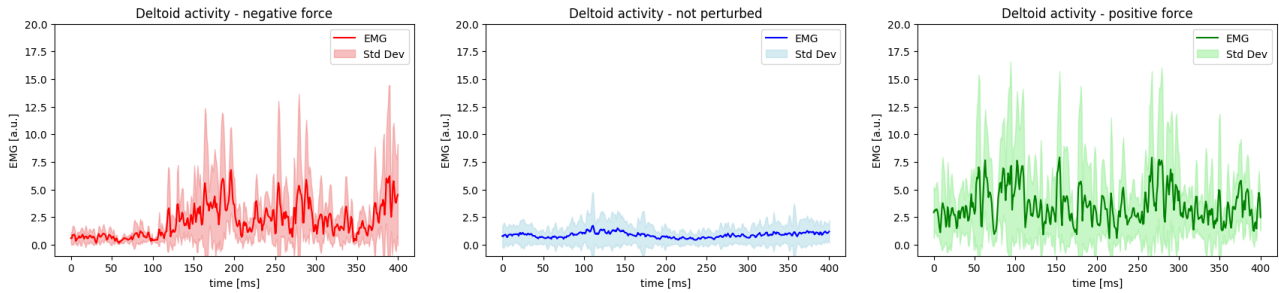


Figure 5: Posterior Deltoid's EMG Data

The deltoid, on the other hand, shows a high activity on both cases. However, in the case of **negative force** it only shows a high peak of activity after 100 ms. This change in the level of activity indicates that the deltoid is indeed needed to counteract the **negative force**.

The **positive force** in figure 3, yields a higher deviation of the movement on the x-axis in comparison to the **negative force**. Correlating this information with the values shown in figures 4 and 5, the observer can deduce that the pectoralis is probably weaker than the deltoid, and therefore less capable to counteract an abduction movement.

3.2 Relationship between EMG and Force applied by the Subject

When it comes to the relationship between the force applied by the subject, it is defined that if the force applied to the subject is of the $F_x = 13\dot{y}$ nature (**positive force**) then the recorded force is negative. For every other type of force it is positive, since **negative force** is of the type $F_x = -13\dot{y}$ and **not perturbed** is a modality that doesn't apply abductions to the subject's arm.

Starting with **negative force** the force applied by the subject steadily increases until it reaches a peak where it starts decreasing. The constant increase of force applied gives a picture on how the subject's deltoid is actuating with more intensity in the subject's arm, reaching a peak when both the pectoralis and the deltoid start working in tandem for the adduction movement, counteracting the force of the robot. In the end, at around 300 ms, the force applied decreases showing that the subject is actively trying to prevent overshoot on his trajectory and beginning his course-correction to the target.

For the **not perturbed** modality, the subject's force has a similar evolution as the subject's deltoid activity. In fact, when the arm is performing an abduction movement, and therefore the deltoid has to contract to a higher level, the patient is applying a positive force on the robotic

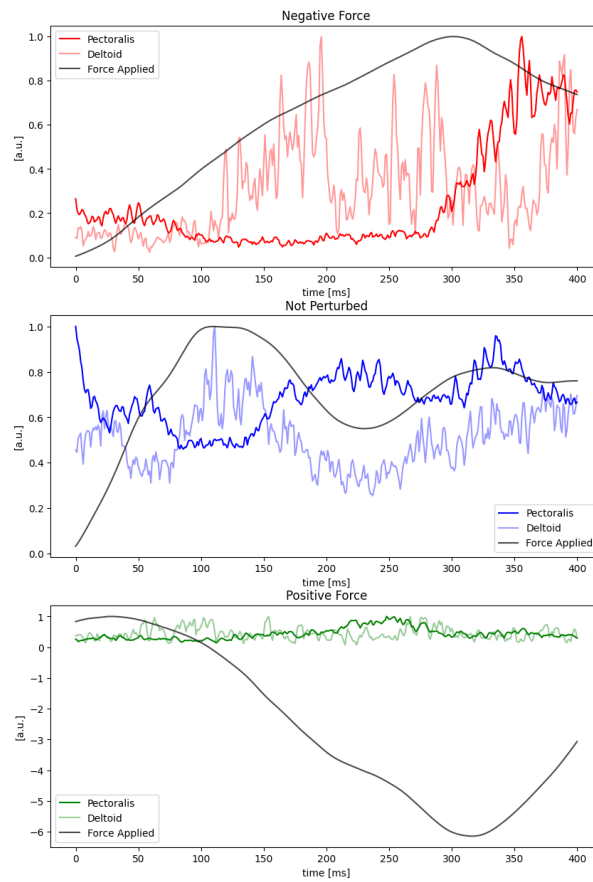


Figure 6: EMG and Force Comparisons (normalized values)

arm, which is the force measured and represented here.

Finally for the **positive force** when considering the absolute value of the applied force, it follows a similar progression as of the one of the **negative force**. It reaches a higher peak, at 6 a.u, due to the fact that, as shown in 3, the **positive force** has a higher deviation than the **negative force**.

Moreover, as shown in figure 3, the subject overshoots in both cases in the end of the trajectory. The reason of this overshoot is evident in figure 7, where both velocities and forces applied by the patient are represented. In the first plot it is shown that the velocity components on x change sign multiple times. Both in the **positive** and in the **negative** case, the velocity changes sign 2 times, where the last peak indicates the corrective movement for the overshoot. From the first column of graphs, it's evident that the trials with **positive** external force have higher velocity peaks and higher force values, with respect to the baseline given by the **not perturbed** modality. This represents the higher deviation on the x axis shown in figure 3, and also in the trends of the y components of the velocities. The **positive force** modality shows in fact a higher velocity, which will therefore create a higher force applied by the robot ($F_x = 13\dot{y}$). The bottom right plot shows that the forces of the patient on y follow the same trends as the velocities, not giving much information about the muscle activation.

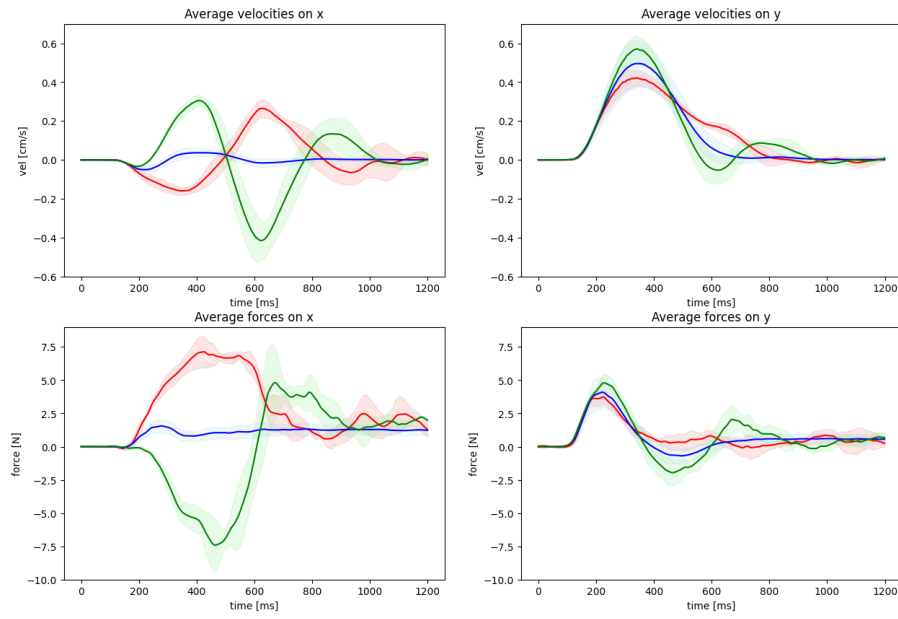
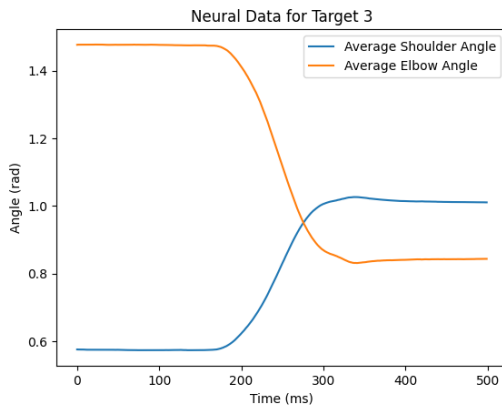


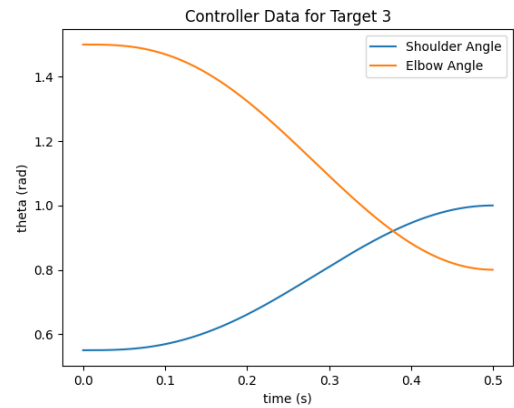
Figure 7: Average Velocities and Forces on x and y components.

4 Stochastic Optimal Control

Looking at the neural data, figure 2, we can see that the shoulder angles for the different targets usually begin at around $\frac{2\pi}{11} \approx 0.55$, while the elbow angles begin at $\frac{\pi}{2} \approx 1.5$. Making use



(a) Neural Data for Shoulder and Elbow for Target 3



(b) Controller Data for Shoulder and Elbow for Target 3

Figure 8: Real Data and Stochastic Controller Data Comparison

of the one joint stochastic optimal controller, as developed before, we can see how starting at $(\frac{2\pi}{11}, \frac{\pi}{2}, 0, 0)$ for the shoulder, elbow angle and angular velocities would affect the end coordinates when reaching for the same targets. In this case the evolution for the targets is similar as to the ones developed by the controller. This means that the one joint controller approximates well the real neural data extracted from the subject.